Appl Petrochem Res (2016) 6:217–223
DOI 10.1007/s13203-016-0154-1

ORIGINAL ARTICLE

Application of Ni–Al-hydrotalcite-derived catalyst modified with Fe or Mg in CO_2 methanation

Xiaolong Wang[1] · Tao Zhen[2] · Changchun Yu[2]

Received: 27 January 2016 / Accepted: 17 May 2016 / Published online: 7 June 2016

Abstract In this work, Ni–Al-hydrotalcite-derived catalyst modified with Fe or Mg for CO_2 methanation was investigated in an attempt to improve the reaction activity at low temperature. Through the characterization of XRD, H_2-TPR, and N_2-BET, 0.05Fe–Ni–Al_2O_3-HT catalyst can be found with a better reducing property, higher surface area, better Ni dispersion, and smaller pore size. The CO_2 conversion using this catalyst was tested in a fixed-bed reactor in laboratory. The result showed better reaction activity at low temperature. At 219 °C, the CO_2 conversion could reach 80.8 %. Meanwhile, the highest CO_2 conversion of 96.0 % was achieved at 350 °C.

Keywords CO_2 methanation · Ni–Al hydrotalcite · Activity · Reducibility · Larger/smaller pore size

List of symbols

λ	X-ray wavelength
θ	Bragg's angle of diffraction
X_{CO_2}	CO_2 conversion
S_{CH_4}	Selectivity of CH_4

Introduction

Global warming resulting from the CO_2 emitted from combustion of fossil fuel is a critical challenge for human beings. Recent studies indicate a high probability of a link between anthropogenic greenhouse gas emissions and observed effects on sea level rising [1], precipitation patterns [2], and ocean acidification [3]. There are three main strategies for reducing CO_2 emission, including increase of renewable energy [4], CO_2 capture and storage [5], and utilization of CO_2 [6]. Hydrogenation of CO_2 is an attractive C1 building block for making organic chemicals, materials, and carbohydrates (i.e., foods). This kind of utilization of CO_2 technology could be a solution to mitigate the global warming. CO_2 as a chemical feedstock in current industrial processes is limited. So far, CO_2 is only used in synthesis of urea and its derivatives, salicylic acid and carbonates. This limitation is due to the thermodynamic stability of CO_2 [7], which requires high energy substances to transform it into other chemicals. Hydrogen can be used as a high energy material for transformation. The hydrogenation of CO_2 can produce more useful fuels and chemicals. Currently, the products of CO_2 hydrogenation being researched include carbon monoxide, methane, methanol, ethanol or higher alcohol, hydrocarbons, dimethyl ether, formic acid, formates, and formamides [8–11]. Some of these products can be used as fuels in internal combustion engines and as raw materials and intermediates in many chemical industries. Moreover, they can be easily liquefied allowing for easy storage and transportation. Last, but not the least, in general, they are more valuable than CO_2.

In recent years, hydrogen production from biomass has received people's attention, and this process can provide abundant H_2 for CO_2 methanation.

The methanation of carbon dioxide, also known as the Sabatier reaction for over a century, has received more interests due to its usage as chemical storage of the excess H_2 generated from renewable energy. The reactions of CO_2 methanation involve several species, such as CO_2, H_2,

✉ Changchun Yu
yucc@cup.edu.cn

[1] Huaneng Clean Energy Research Institute, Beijing 102209, China

[2] China University of Petroleum, Beijing, China

CH_4, H_2O, C^{2+}, and CO. The main mechanism of this system can be described by the following three reactions.

$$CO_2 + H_2 = CH_4 + 2H_2O\ \Delta H\,(298\ \mathrm{K}) = -165\ \mathrm{kJ/mol} \quad (1)$$

$$CO_2 + H_2 = CO + H_2O\ \Delta H\,(298\ \mathrm{K}) = 41\ \mathrm{kJ/mol} \quad (2)$$

$$xCO_2 + yH_2 = C_xH_{(y-4x)} + 2xH_2O \quad (3)$$

As can be seen from the ΔH, the reaction (1) is a strong exothermic process. For the adiabatic fixed-bed reactor, the temperature can rise 61 °C for every 1 % conversion of CO_2 [12]. To reduce the heating effect of the reaction, the process of product gas recirculation has to be applied [13–15].

High CH_4 yields can only be achieved when a catalyst is applied [16, 17]. Ru [18], although more efficient, is quite expensive and presents a significant cost barrier to its commercial application. Therefore, supported nickel catalysts remain the most widely investigated ones due to their high efficiency in CH_4 production and low cost. However, Ni-based catalysts are not selective and are subject to be coking, which lowers the efficiency of methanation. Lei et al. found that Ni–Al-hydrotalcite-derived catalyst with well-dispersed Ni particles and strong basic sites showed excellent performance for CO_2 methanation [19]. Shohei et al. pointed out that CeO_2 could reduce the particle size of catalyst Ru/Al_2O_3 [20]. Huailiang et al. proved that ZrO_2 could promote the dispersion of Ni on catalyst support and provide larger activity area [21]. Takano et al. pointed that ZrO_2 could provide oxygen vacancy for CO_2 adsorption so as to enhance the activity of catalyst [22].

In theory, when CO_2 is hydrogenated, the CO_2 firstly converts into carbonate or bicarbonate, and the H_2 is dissociated into hydrogen atom. Then, the carbonate or bicarbonate is hydrogenated and loses H_2O step by step. Finally, the CH_4 is formed and leaves the catalyst surface [23]. The catalyst with proper H_2 and CO_2 adsorption shows the best activity in the process of CO_2 methanation. It has been found that the capacity of H_2 adsorption on polycrystalline of Fe is better than that of Ni. So, the catalyst could be modified with Fe to enhance the adsorption of H_2. To enhance the adsorption of CO_2, the catalyst could be modified with Mg for its alkalinity.

In this work, Ni–Al-hydrotalcite-derived catalyst modified with Fe or Mg by co-precipitation method introduced by Lei was applied in the CO_2 methanation [19]. On this basis, the urea instead of NaOH and $NaCO_3$ was used as precipitant to avoid the introduction of Na ions. And the influences of different content of Fe or Mg and reaction temperature on CO_2 conversion were studied.

Experimental

Catalyst preparation

The precursor of the catalyst was prepared by co-precipitation method with urea. Briefly, 0.03 mol $Ni(NO_3)_2{\cdot}6H_2O$, 0.015 mol $Al(NO_3)_3{\cdot}9H_2O$, and 0.18 mol $CO(NH_2)_2$ were added into a 500-ml three-mouth flask, then mixed and dissolved with 500 ml deionized water. Afterward, the solution was kept at 100 °C for 24 h to obtain a precipitate with Ni–Al hydrotalcite structure. After filtering, washing, and drying at 80 °C for 24 h, the obtained hydrotalcite was reduced at 700 °C for 4 h to get the Ni–Al_2O_3-HT catalyst.

The catalyst modified by Fe or Mg was prepared according to the above-mentioned method with one more process of adding material. $Fe(NO_3){\cdot}9H_2O$ was added into the mixture to obtain the Fe–Ni–Al_2O_3-HT catalyst with desired Fe loading amount. It was denoted as 0.05Fe–Ni–Al_2O_3-HT and 0.25Fe–Ni–Al_2O_3-HT, which showed the mole ratio of $Fe(NO_3){\cdot}9H_2O$ and $Al(NO_3)_3{\cdot}9H_2O$ as 0.05 and 0.25, respectively. Similarly, $Mg(NO_3)_2{\cdot}6H_2O$ was added into the mixture to obtain Mg-modified catalyst. And the catalysts were named 0.1MgO–Ni–Al_2O_3-HT and 1MgO–Ni–Al_2O_3-HT catalysts according to different Mg loading amount.

Experimental setup

The catalytic performance for CO_2 hydrogenation to CH_4 was evaluated in a continuous-flow fixed-bed reactor at 2 MPa. 1.000 g catalyst (20–40 mesh) was loaded in the reactor. The catalyst was firstly reduced with H_2 (75 ml/min) at 700 °C for 4 h. Then, the reactor was cooled down to 100 °C in H_2. The feed gas of 19 vol % CO_2, 76 vol % H_2, and balanced with 5vol %N_2 was supplied at a total flow rate of 200 ml/min. Then, the reactor was heated from 100 to 700 °C at 2 °C/min and kept for 1 h every 50 °C. Finally, the products passed through a cold trap (1 °C) and they were analyzed by the GC (7890B, Agilent). The CO_2 conversion and methane selectivity were calculated as follows:

$$CO_2\ \text{conversion: } X_{CO_2}(\%) = \frac{V_{CO_2 in} - V_{CO_2 out}}{V_{CO_2 in}} \times 100\ \%$$

$$CH_4\ \text{selectivity: } S_{CH_4}(\%) = \frac{V_{CH_4 out}}{V_{CO_2 in} - V_{CO_2 out}} \times 100\ \%$$

$$CH_4\ \text{yield: } Y_{CH_4}(\%) = \frac{X_{CO_2} S_{CH_4}}{100} = \frac{V_{CH_4 out}}{V_{CO_2 in}} \times 100\ \%$$

Characterization

X-ray power diffractometer (RigakuD/max 2500) with Cu Kα radiation ($\lambda = 0.154056$ nm) was performed to determine the bulk crystalline phase of the catalyst. The XRD

data were recorded with a scanning speed of 10°/min in the range of 10°–90°.

H_2-TPR (Micromeritics 2720) was used to investigate the reducibility of the nickel on catalysts. The samples (0.1 g) were pre-dried at 350 °C in He flow (30 ml/min) for 30 min. Then, the samples were heated to 900 °C at a rate of 10 °C/min in 10 vol % H_2-Ar (25 ml/min).

Nitrogen adsorption–desorption isotherms were recorded using a Quantachrome 3QDS-MP-30 instrument. The total surface area was determined according to the BET equation. The pore size distribution was determined using DFT method.

Result and discussion

Once the catalyst precursors were reduced, the Ni grain can burn with the oxygen in the air, which can destroy the surface structure of catalyst. The catalyst precursors were used for characterization to avoid the destruction.

Figures 1 and 2 showed the XRD patterns of the different catalyst precursors. Apparent diffraction bands at 37.2°, 43.3°, 63.0°, 75.3°, and 79.5° were observed, which corresponded to the diffraction of lattice planes of 111, 200, 220, 311, and 222 of nickel oxide. It can be seen that the catalyst precursors modified with a small amount of Fe and Mg showed no obvious peaks of NiO, which means the crystallinity of NiO becomes lower. Once the catalyst precursors were reduced, these catalysts could have a good Ni dispersion. Hence, the proper introduction of Fe or Mg can benefit the Ni dispersion and prevent the crystal growth of NiO particles for Ni–Al-hydrotalcite-derived catalyst precursor. However, a slightly stronger diffraction peak was found in 1MgO–NiO–Al_2O_3-HT compared with

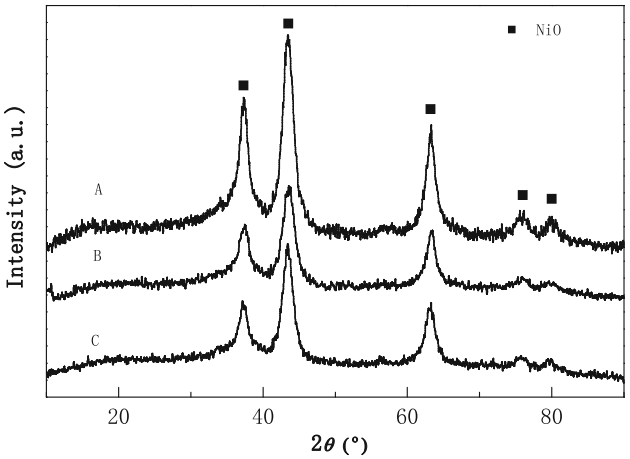

Fig. 2 XRD patterns of the methanation catalyst precursors at different Mg loading level *A* 1 MgO–NiO–Al_2O_3-HT, *B* 0.1 MgO–NiO–Al_2O_3-HT and *C* NiO–Al_2O_3-HT

0.1MgO–NiO–Al_2O_3-HT. This means the modification with Mg at high loading level can weaken Ni dispersion.

Figure 3 showed the H_2-TPR profiles with different Fe loading levels. A broad H_2 consumption peak between 400 and 800 °C was found for these catalyst precursors. Specifically, two reduction desorption peaks were detected on these catalyst precursors. The first peak located at 418 °C for NiO–Al_2O_3–HT, 380 °C for 0.05 Fe_2O_3–NiO–Al_2O_3-HT, and 358 °C for 0.25 Fe_2O_3–NiO–Al_2O_3-HT. With the increase of Fe loading, the reduction temperature decreased from 660 to 518 °C, while the area of the H_2 desorption became larger. Meanwhile, the deduction temperature of the second peak decreased from 721 to 688 °C, while the area of the TCD signal became smaller. The first reduction peak represented the reduction of NiO as shown in Fig. 1. And the second reduction peak represented the

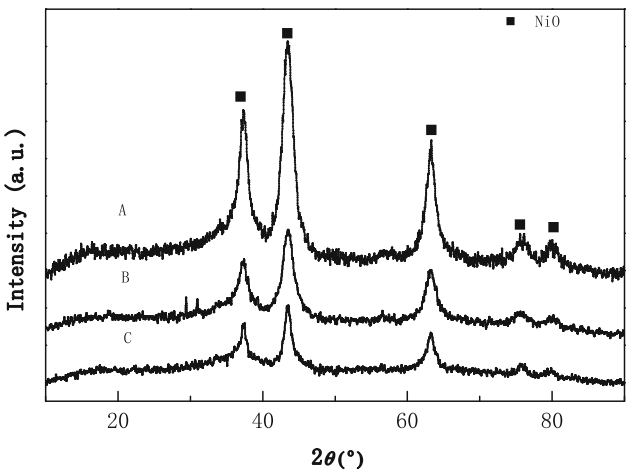

Fig. 1 XRD patterns of the methanation catalyst precursors at different Fe loading level *A* 0.25 Fe_2O_3–NiO–Al_2O_3-HT, *B* 0.05 Fe_2O_3–NiO–Al_2O_3-HT and *C* NiO–Al_2O_3-HT

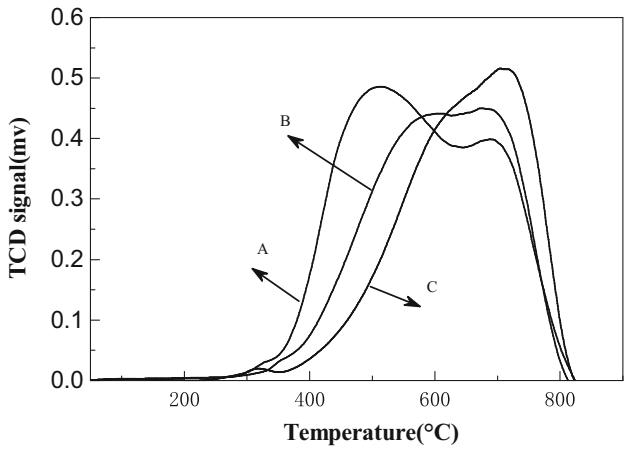

Fig. 3 H_2-TPR profiles of catalyst precursors at different Fe loading level *A* 0.25 Fe_2O_3–NiO–Al_2O_3-HT, *B* 0.05 Fe_2O_3–NiO–Al_2O_3-HT and *C* NiO–Al_2O_3-HT

layered composite oxides generated after the calcination of hydrotalcite [24]. The existence of the Fe iron with different ionic radius prevented the growing up of the structure of hydrotalcite. In consequence, it can enhance the reducibility of the catalyst.

As is shown in Fig. 4, catalyst precursors modified with Mg showed different effects with Fe. Compared with Ni–Al-hydrotalcite-derived catalyst, the reduction peaks of 0.1 MgO–NiO–Al_2O_3-HT catalyst precursor moved about 10 °C to the higher temperature range. However, the area of the TCD signal became slightly larger. Meanwhile, the reduction peaks of 1 MgO–NiO–Al_2O_3-HT catalyst precursors showed an apparent difference with other catalyst precursors. The area of the TCD signal became apparently smaller. This suggested that the modification with Mg at high loading level reduced its reducibility. Therefore, the modification with Mg at high loading level can enhance the interaction of nickel with other components in catalyst precursors.

NiO–Al_2O_3-HT catalyst precursor showed a relatively high specific surface area($s = 125$ m^2/g) as shown in Table 1. NiO–Al_2O_3-HT catalyst precursor showed wide range of pore distribution at the entire measuring range (1–22 nm). The catalyst precursor modified with Fe mainly showed micropores of 1.5 nm and mesopores of 3.0 and 5.0 nm. No mesopores over 7.0 nm were observed in Fig. 5. As for Ni–Al-hydrotalcite-derived catalyst modified with Mg, there was a difference. On the one hand, the catalyst precursor showed similar distribution above 4.5 nm with NiO–Al_2O_3-HT catalyst precursor. On the other hand, 0.1 MgO–NiO–Al_2O_3-HT catalyst precursor showed micropores of 1.5 nm and mesopores of 3.0 nm in Fig. 6; while the mesopores mostly distributed around 5.0 nm for 1 MgO–NiO–Al_2O_3-HT catalyst precursor.

It could be concluded from Table 1 and Figs. 5 and 6 that the introduction of a proper amount of Fe or Mg to the Ni–Al-hydrotalcite-derived catalyst could change the pore distribution and generate more pores under 7.0 nm. Therefore, the catalyst precursor showed a high specific surface area, while excessive Fe or Mg had negative effect on the catalytic property and performance.

To enhance the adsorption of H_2, Fe was introduced into Ni–Al-hydrotalcite-derived catalyst. Figures 7 and 8 showed the effect of temperature on the CO_2 conversion and CH_4 selectivity of CO_2 hydrogenation reaction under different conditions. For these catalysts, the methanation reaction started up from 150 °C and generated CH_4. When the temperature of reaction was increased gradually, the CO_2 conversion increased rapidly at first, and if the temperature was over about 400 °C, the CO_2 conversion began to drop due to the restriction by thermodynamic

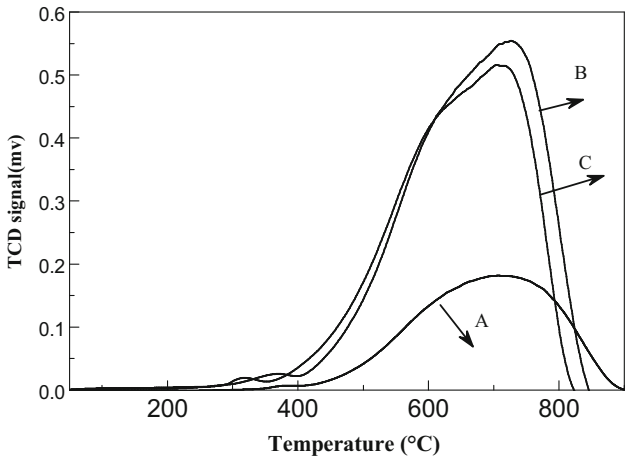

Fig. 4 H_2-TPR profiles of catalyst precursors at different Mg loading level *A* 1 MgO–NiO–Al_2O_3-HT, *B* 0.1 MgO–NiO–Al_2O_3-HT and *C* NiO–Al_2O_3-HT

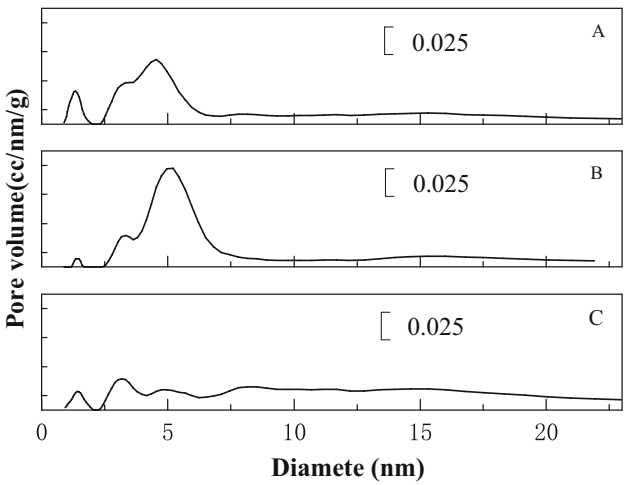

Fig. 5 N_2-BET profiles of Fe_2O_3–NiO–Al_2O_3-HT catalyst precursors at different Fe loading level *A* 0.25 Fe_2O_3–NiO–Al_2O_3-HT, *B* 0.05 Fe_2O_3–NiO–Al_2O_3-HT and *C* NiO–Al_2O_3-HT

Table 1 The microscopic property of catalyst precursors

Catalyst precursors	NiO–Al_2O_3-HT	0.05 Fe_2O_3–NiO–Al_2O_3-HT	0.25 Fe_2O_3–NiO–Al_2O_3-HT	0.1 MgO–NiO–Al_2O_3-HT	1 MgO–NiO–Al_2O_3-HT
Surface area (m^2/g)	125	153	142	166	124
Pore volume (cc/g)	0.86	0.53	0.59	1.17	1.18

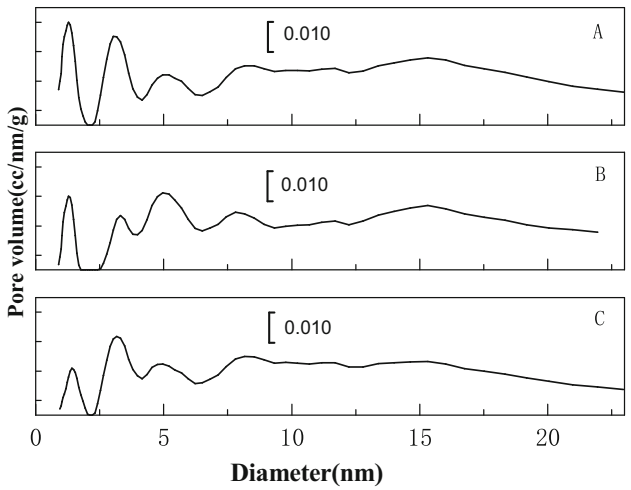

Fig. 6 N_2-BET profiles of MgO–NiO–Al_2O_3 catalyst precursors at different Mg loading level *A* 1MgO–NiO–Al_2O_3-HT, *B* 0.1 MgO–NiO–Al_2O_3-HT and *C* NiO–Al_2O_3-HT

equilibrium. The highest CO_2 conversion of 96.0 % was observed at about 350 °C. And the selectivity of CH_4 remained nearly 100.0 % below 500 °C, then began to reduce with the further increase of reaction temperature. Specifically, the temperature raised a step further, CO was observed in this process.

Comparing the three catalysts, it could be seen that the modification of Fe can apparently improve catalytic activity under 300 °C. The CO_2 conversion with the Ni–Al_2O_3-HT catalyst just reached 16.4 % at 206 °C. After modified with Fe, the CO_2 conversion reached 80.8 % at 219 °C using the 0.05 Fe–Ni–Al_2O_3-HT catalyst and 81.0 % at 222 °C using the 0.25 Fe–Ni–Al_2O_3-HT catalyst. Fe was also the active component of Fischer-Tropsch synthesis, so the ethane was observed at 200–300 °C. What is more, the proportion of ethane increased with the increase of Fe loading amount.

To enhance the adsorption of CO_2, Mg was introduced into the Ni–Al-hydrotalcite-derived catalyst. Figure 9 shows the effect of Mg on the catalytic performance of the CO_2 methanation process. 0.1 MgO–Ni–Al_2O_3-HT catalyst showed the best low-temperature activity below 300 °C. The CO_2 conversion reached 71.4 % at 213 °C using 0.1 MgO–Ni–Al_2O_3-HT. It was higher than Ni–Al_2O_3-HT catalyst with 16.4 % CO_2 conversion at 206 °C and 1 MgO–Ni–Al_2O_3-HT catalyst with 14.9 % CO_2 conversion at 210 °C. When the temperature was higher than 300 °C, there was almost no difference between these three kinds of catalysts. Figure 10 shows the selectivity of the three different kinds of catalysts, the CH_4 selectivity was over 99.0 % under 500 °C, and began to fall since 500 °C for CO generation.

Briefly, proper amount of Mg could enhance catalyst alkaline, and then accelerated CO_2 conversion under

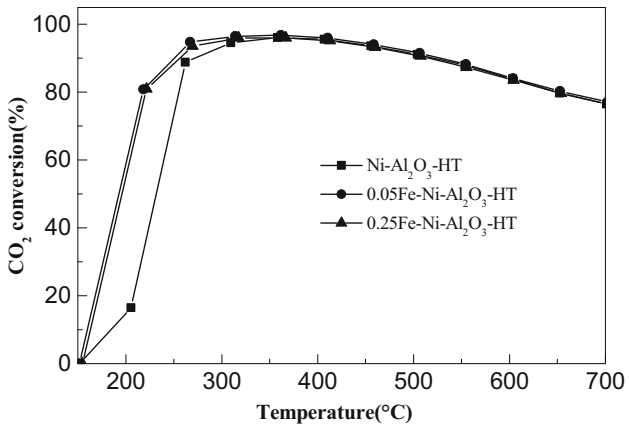

Fig. 7 Effect of reaction temperature on CO_2 conversion over Fe–Ni–Al_2O_3-HT catalysts

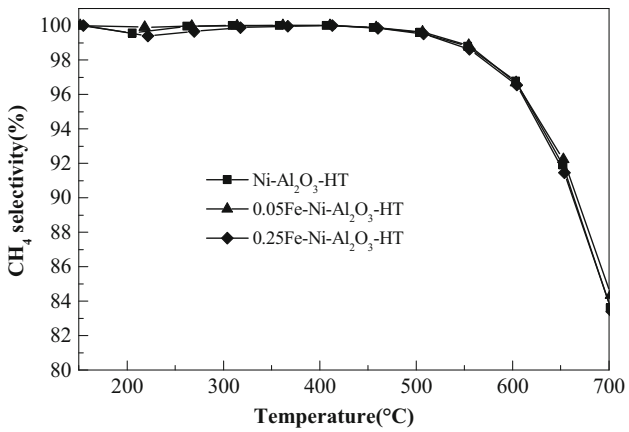

Fig. 8 Effect of reaction temperature on CH_4 selectivity over Fe–Ni–Al_2O_3-HT catalysts

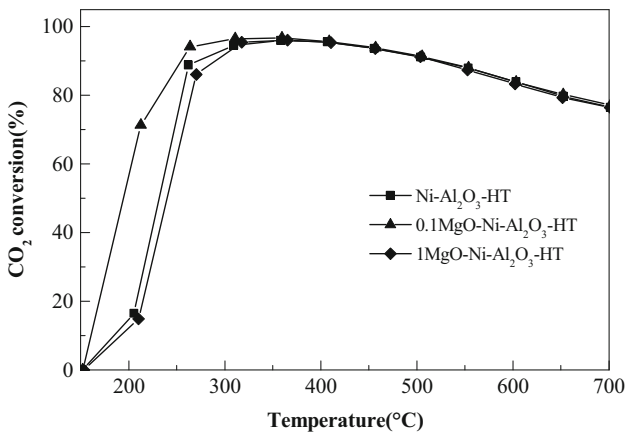

Fig. 9 Effect of reaction temperature on CO_2 conversion over Fe–Ni–Al_2O_3-HT catalysts

300 °C. The catalyst became difficult to restore as shown in Fig. 10, and the CO_2 conversion was reduced at high temperature.

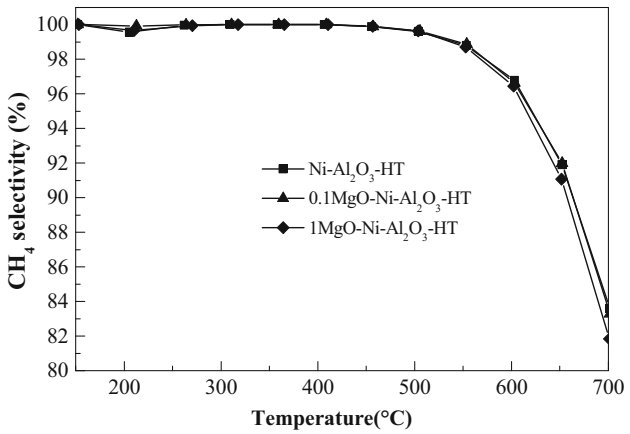

Fig. 10 Effect of reaction temperature on CH_4 selectivity over Fe–Ni–Al_2O_3-HT catalysts

Conclusion

Ni–Al-hydrotalcite-derived catalyst modified with Fe or Mg for CO_2 methanation was investigated to improve the reaction activity at low temperature. It was found that proper amount of Fe could enhance the dispersion of NiO, improve the reducibility, and change the pore distribution. In consequence, the low-temperature activity was also significantly improved. The reaction started at 200 °C using 0.05 Fe–Ni–Al_2O_3-HT catalyst, which was 50 °C lower than that using Ni–Al_2O_3-HT catalyst without modification. And the CH_4 selectivity could reach 100.0 % at 362 °C at the CO_2 conversion of 96.8 %. The catalyst was also modified with Mg to enhance the adsorption capacity of CO_2. And it showed the same effect for the dispersion of NiO. But, the catalyst became difficult to be reduced and had no obvious improvement in the pore distribution. What is more, the catalytic activity of the catalyst modified with Mg at low temperature was lower than the one modified with Fe.

Acknowledgments This work received support from Beijing Municipal Science and Technology Commission (Z151100002815009).

References

1. Daniel A, Lashof Dilip R, Ahuja (1990) Relative contributions of greenhouse gas emissions to global warming. Lett Nat 5(4):529–531
2. Stefan JF, Michel K, Berthold H, Baumgarten A, Wanek W (2012) Influence of altered precipitation pattern on greenhouse gas emissions and soil enzyme activities in Pannonian soils. Geophy Res Abst 15(11):438
3. Alex K (2014) We're Running Out of Time: Ocean Acidification and Greenhouse Gas Emissions Soar. Climate News Network (9)
4. Paul B (2008) Coping with carbon: a near-term strategy to limit carbon dioxide emissions from power stations. Philosoph Trans Royal Soc 366(8):3891–3900
5. Leung Dennis Y C, Caramanna G, Maroto-Valer M (2014) An overview of current status of carbon dioxide capture and storage technologies. Renew Sustain Energy Rev 39(11):426–443
6. Tim R (2013) Waste CO_2 could be source of extra power. Sci Am 16(8):57
7. Torsten R, Plugge CM, Abram NJ, Judy H (2008) Reversible interconversion of carbon dioxide and formate by an electroactive enzyme. Curr Issue 105:10654–10658
8. Jadhav SG, Vaidya PD, Bhanage BM, Joshi B (2014) Catalytic carbon dioxide hydrogenation to methanol: a review of recent studies. Rev Article 92(11):2557–2567
9. Ratchprapa S, Koizumi N, Prasassarakich P (2013) Bimetallic Fe–Co catalysts for CO_2 hydrogenation to higher hydrocarbons. Int J CO_2 Util 3–4:102–106
10. Wengui G, Hua W, Yuhao W, Wei G, Miaoyao J (2013) Dimethyl ether synthesis from CO_2 hydrogenation on La-modified CuO–ZnO–Al_2O_3/HZSM-5 bifunctional catalysts. J Rare Earths 31(5):470–476
11. Huff CA, Sanford MS (2013) Catalytic CO_2 hydrogenation to formate by a ruthenium pincer complex. Acs Catal 3(3):2412–2416
12. Yubang Z (2011) The thermodynamic analysis of syngas to substitute natural gas. Chem Ind Eng 28(6):47–53
13. Hoehlei B (1984) Methane from synthesis gas and operation of high-temperature methanation. Nucl Eng Des 78(2):241–250
14. Shinnar R (1982) Thermodynamic and kinetic constraints of catalytic synthetic natural gas processes. Ind Eng Chem Process Des Dev 21(4):728–750
15. Allen R, Billinton R, Lee SH (1988) Bibliography on the application of probability methods in power system reliability evaluation IEEE Winter Meeting (C)
16. Beuls A, Swalus C, Jacquemin M, Heyen G, Karelovic A (2012) Methanation of CO_2: further insight into the mechanism over Rh/γ-Al_2O_3 catalyst. Appl Catal B Environ 113–114:(2–10)
17. José L, Manuel FR, Pereira et al (2013) Synthesis and functionalization of carbon xerogels to be used as supports for fuel cell catalysts. J Energy Chem 2(11):195–201
18. Eckle S, Anfang HG, Behm J (2011) Reaction Intermediates and Side Products in the Methanation of CO and CO_2 over Supported Ru Catalysts in H_2-Rich Reformate Gases. J Phy Chem 115(4):1361–1367
19. Lei H, Lin Q, Huang Y (2014) Unique catalysis of Ni-Al hydrotalcite derived catalyst in CO_2 methanation: cooperative effect between Ni nanoparticles and a basic support. J Energy Chem 23(4):587–592
20. Tada S, Ochieng OJ, Kikuchi R, Haneda T, Kameyama H (2014) Promotion of CO_2 methanation activity and CH_4 selectivity at low temperatures over Ru/CeO_2/Al_2O_3 catalysts. Sci Direct 39:10090–10100
21. Lu H, Yang X, Gao G, Wang K, Shi Q (2014) Mesoporous zirconia-modified clays supported nickel catalysts for CO and CO_2 methanation. Int J Hydrogen Energy (39):18894–18907
22. Takano H, Shinomiya H, Lzumiya K, Kumagai N, Habazaki H (2015) CO_2 methanation of Ni catalysts supported on tetragonal ZrO_2 doped with Ca^{2+} and Ni^{2+} ions. Int J Hydrogen Energy (40):8347–8355

23. Ussa Aldana PA, Ocampo F, Kobl K, Louis B, Thibault-Starzyk F, Daturi M (2013) Catalytic CO_2 valorization into CH_4 on Ni-based ceria-zirconia. Reaction mechanism by operando IR spectroscopy. Catal Today 10:215

24. Feng JT, Lin YJ, Evans DG, Li DQ (2009) Enhanced metal dispersion and hydrodechlorination properties of a Ni/Al_2O_3 catalyst derived from layered double hydroxides. J Catal 266(2):351–358